Influence of Satellite Imaging Geometry on ASTER and SRTM Global Digital Elevation Models

Foumelis M.[1], Chalkias C.[2] and Plank S.[3]

[1] *RSAC c/o, Science, Applications and Future Technologies Department, Directorate of EO Programmes, European Space Agency (ESA-ESRIN), Via Galileo Galilei, 00044 Frascati, Rome, Italy,* michael.foumelis@esa.int

[2] *Department of Geography, Harokopio University, 70 El. Venizelou Str., 17671 Kallithea, Athens, Greece,* xalkias@hua.gr

[3] *German Remote Sensing Data Center (DFD), German Aerospace Center (DLR), 82234 Oberpfaffenhofen, Germany,* simon.plank@dlr.de

Abstract

In this paper we assess the accuracy of ASTER and SRTM height estimates, investigating the spatial distribution of their deviations from a reference height dataset derived from topographic maps. The analysis is performed over the hydrological basin of the Xerias River located at the northeastern part of Peloponnesus. The selected area exhibits complex terrain allowing for the detailed evaluation of the influence of local topography on the satellite height estimates. The aim was to identify regions where deviations exist, recognize potential spatial patterns and verify whether they are controlled or not by specific morphological parameters. The investigation included geostatistical analysis of height differences with respect to parameters such as elevation, slope gradient, slope aspect and morphological units. Regression analysis results showed both systematic and non-systematic trends. For ASTER the deviations are limited to a global shift, while of importance is the positive correlation between the spatial distributions of deviations and aspect for the SRTM model. Further analysis included simulation of the SRTM imaging geometry to support understanding of the observed height deviation. It was verified that the sign and magnitude as well as the location of the deviations are related to the methods of height extraction from space-borne systems, being more pronounce in the SRTM model as a result of the side looking configuration of SAR sensors. These findings underline that the source of deviations in satellite derived height models should not be fully attributed to local morphological characteristics, since space-borne imaging is contributing significantly, paving the way for a more adequate utilization of these global elevation models.

Keywords: ASTER, SRTM, Height Deviations, Spatial Patterns, SAR Imaging Simulation, GIS Geostatistical Analysis

1. Introduction

Over the past years global Digital Elevation Models (DEMs) derived from sensors on-board satellite platforms, such as the Shuttle Radar Topography Mission (SRTM) and the Advanced Spaceborne Thermal Emission and Reflection Radiometer (ASTER) have been released, covering almost the entire globe. These models are continuously updated by applying several post-processing enhancement steps including filling data gaps, pits and spike removal and definition of water body extent (Werner 2001).

Nowadays, there is a growing interest for these global elevation models, as they implicate various disciplines related to geohazards (e.g. earthquakes, landslides, floods, tsunami etc.), with significant socio-economic impact. In this context global datasets serve not only scientific goals as a fundamental input to a wide range of applications (ortho-rectification, SAR interferometry, landslide modelling, etc.), but also to policy and decision making. With the advent of more advanced satellite sensors a trend towards height models of ever increasing resolution is clearly evident. Realization of dedicated mission such as DLR's TanDEM-X mission, building on modern radar imaging technology, is an example.

While conventional topographically derived DEMs are still of importance mainly due to their resolution and accuracy, free availability of global sets allowed further exploitation.
Besides the spatial coverage, among their advantages are the uniform georeferencing and the common processing, providing uniformity within the dataset. That enabled their direct use in a significant number of geoscience applications, among which wide scale geomorphological and neotectonic mapping, hydrological modelling and flood hazard simulation, lava flow forecasts in volcanic hazard models and removal of topography contribution in SAR interferometry, as well as a wide range of applications related to geodetic and atmospheric sciences.
Nonetheless, questions are being raised regarding the actual and not the foreseen theoretical accuracy of these global DEMs, leading to extensive assessment of their properties by various research groups and institutions. The problem is two folded and involves the accuracy of the height estimates themselves, as well as the geolocation accuracy of these global datasets.
Concerning the geolocation accuracy of satellite derived DEMs, outside the focus of the present investigation, it depends on a number of processing parameters and the information extraction technique implemented, as well as on the local morphological conditions (Van Niel et al. 2008; Rawat 2013), rendering them partly case specific.
The assessment of the vertical accuracy of global height models has been investigated in previous studies, either directly using GPS measurements, leveling campaigns or other height estimates (Mouratidis et al. 2010; Sharma et al. 2010; Gómez-Gutiérrez et al. 2011), or by comparisons to selected reference datasets (Nikolakopoulos and Chrysoulakis 2006; Nikolakopoulos et al. 2006; Miliaresis 2007). In the first case, highly accurate height estimates are considered, providing robust indications of the overall expected deviations of the datasets, limited though by the point sampling. In the second group of studies on the contrary, spatially continuous assessment is undertaken without necessary providing absolute definitions of the observed relative deviations. In both approaches, results regarding the estimated differences are often presented in the form of basic descriptive statistics. In other cases, focus is given on the spatial properties of these differences, examined in relation to various parameters, such as land cover types, using statistical indicators (Miliaresis 2008). Although the correlation of observed height deviation with terrain characteristics is being already documented (Gorokhovich and Voustianiouk 2006; Shortridge and Messina 2011), specific details on the factors controlling these deviations are not sufficiently described, whereas interpretations are commonly expressed in a more qualitative way.
In the present study the main goal was to identify dependencies, to recognize existing errors in space-borne height models, as well as to understand whether they are controlled or not by terrain characteristics and/or imaging geometry of the satellite sensors. The investigation includes geostatistical analysis based on regression of the heights and height deviations (HD) with respect to parameters, such as elevation, slope gradient, slope aspect and terrain classes, to reveal potential systematic and non-systematic spatial trends. A simulation of the satellite imaging geometry in a Geographic Information System (GIS) was considered to support the understanding of the source of these errors.

2. Background on ASTER and SRTM missions

The Shuttle Radar Topography Mission (SRTM) was conceived as a cooperation of several space agencies and research institutions, the U.S. National Aeronautics and Space Administration (NASA), the Jet Propulsion Laboratory (JPL), the U.S. National Geospatial-Intelligence Agency (NGA) (formerly NIMA), the German Aerospace Center (DLR) and the Agenzia Spaziale Italiana (ASI). During 11^{th} to 22^{th} of February 2000 approximately 80% of the Earth's land surface (ca. 56° S to 60.25° N latitude) was imaged by means of SAR interferometry. Two single-pass interferometers were operated in parallel, the German/Italian X-band system and the U.S. C-band system. The master channels (transmit and receive) of both interferometers were installed in the shuttle cargo, while the secondary antennas (receive only) were mounted on a 60 m long mast. The coverage of the C-SAR is ca. 119 million km^2,

the one of X-SAR ca. 58 million km², with a spatial resolution of 3 and 1 arc seconds, respectively (Rabus et al. 2003).
As part of the SRTM mission, an extensive ground campaign was conducted by NIMA and NASA to collect ground-truth which would allow for the global validation of this unique data set. Details on absolute and relative errors of SRTM can be found in Rodríguez et al. (2005). The C-band elevation model, of about 90 m spatial resolution has a 16 m absolute vertical linear accuracy and 20 m absolute horizontal radial accuracy at 90% (Rabus et al. 2003; https://directory.eoportal.org/web/eoportal/satellite-missions/s/srtm). SRTM DEM is currently available at version 4 (at e.g. http://srtm.csi.cgiar.org).
The Advanced Spaceborne Thermal Emission and Reflection Radiometer (ASTER) was developed as a joint Earth observation project between the U.S. and Japan. ASTER is mounted on Terra mission. The first satellite was launched in December 1999. Additional to its nadir-looking instrument (3N band) ASTER has a backward looking sensor (3B band) receiving in the VNIR channel (0.78 – 0.86 μm) (Abrams 2000). This configuration enables the generation of DEMs by optical stereoscopy at a spatial resolution of 15 m (Hirano et al. 2003; Lee et al. 2003). The maximum error on ground surface is reported as 30 m and the maximum elevation error 15 m (ERSDAC 2003). ASTER GDEM is currently available at version 2 (http://gdem.ersdac.jspacesystems.or.jp).
Since space-borne elevation datasets represent practically the Earth's surface, including vegetation as well as natural and anthropogenic features, their values are referred herein as "heights".

3. Data and analysis

For the purpose of the study an area exhibiting relatively complex terrain was selected, allowing for the detailed evaluation of the influence of the local topography on the satellite height estimates. The area of interest (AOI) is located at the northeastern part of Peloponnesus, Greece and comprises the entire hydrological basin of Xerias River (Fig. 1). A number of past flooding events have been reported in various populated parts of the basin, including the city of Corinth, underlining the importance of accurate height information for regional hydrological modelling purposes (Foumelis 2004).

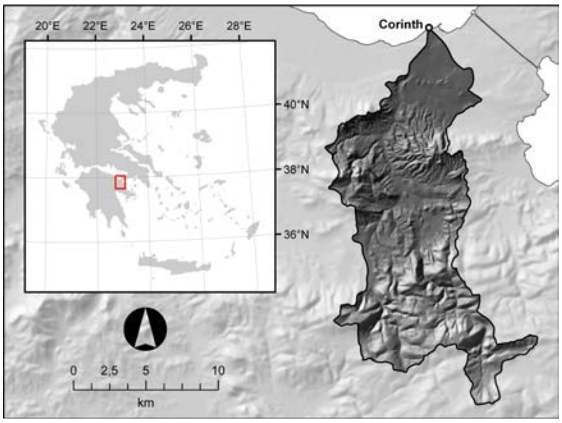

	TOPO30	ASTER G-DEM	SRTM V3	TOPO30–ASTER G-DEM	TOPO30–SRTM V3
Min	0	0	0	-76	-91
Max	1123	1111	1124	112	90
Mean	419.7	408.5	424.5	11.2	-4.6
St Dev	267.2	267.7	267.4	9.8	14.7

Figure 1: Location map of the study area and statistical properties of the examined DEMs (in meters).

Topographic maps were acquired from the Hellenic Military Geographical Service (HMGS), at 1:50,000 scale, presenting nominal horizontal and vertical accuracies of 20 m and 10 m respectively (at 90% confidence). Contour lines with an interval of 20 m as well as point heights were digitized in a Geographic Information System (GIS), whereas for the generation of the reference DEM (hereafter referred to as TOPO30) and during interpolation procedure the drainage network was additionally taken into account. For the interpolation of heights the TOPOGRID algorithm implemented in the ArcGIS software package was used (Hutchinson 1989; 1993), resulting in a hydrologically correct DEM.

The ASTER GDEM was obtained from the EOS data archives of JPL and SRTM V3 elevation data (available release during the study) from the Consortium for Spatial Information (CGIAR-CSI), at a spatial resolution of about 30 m and 90 m respectively. Statistical properties of the examined DEMs and their differences within the region of interest are given in figure 1.

Pre-processing of each individual height model included referencing it to the WGS84/EGM96 reference system. Since SRTM data were already provided in UTM projection, re-projection of ASTER acquired in geographic coordinates was required. Coordinate transformation of the digitized contours and point heights, initially in the GGRS87 projection, to the common map projection was performed before spatial interpolation process to avoid potential resampling errors.

Due to the different spatial resolution, the original datasets had to be resampled to a common spatial grid, over which the analysis would be performed. Subsampling of the various height models to the coarser resolution, namely the 90 m of the SRTM, was considered to reduce artifacts. Thus, based on the SRTM grid the ASTER heights were subsampled based on the bilinear interpolation technique, whereas the TOPO30 DEM was directly sampled to the extent and resolution of SRTM, to ensure accurate pixel overlapping without the intermediate resampling step.

Subsequently, height difference maps from the selected reference using the resampled height models were generated (TOPO30-ASTER and TOPO30-SRTM) (Fig. 2) To facilitate further analysis a slope map and a corresponding aspect map (Travis et al. 1975) were generated from the TOPO30 DEM, as well as a classification of the terrain, by segmenting the area into various terrain classes, namely channels, concave breaks, flats, convex breaks and ridges.

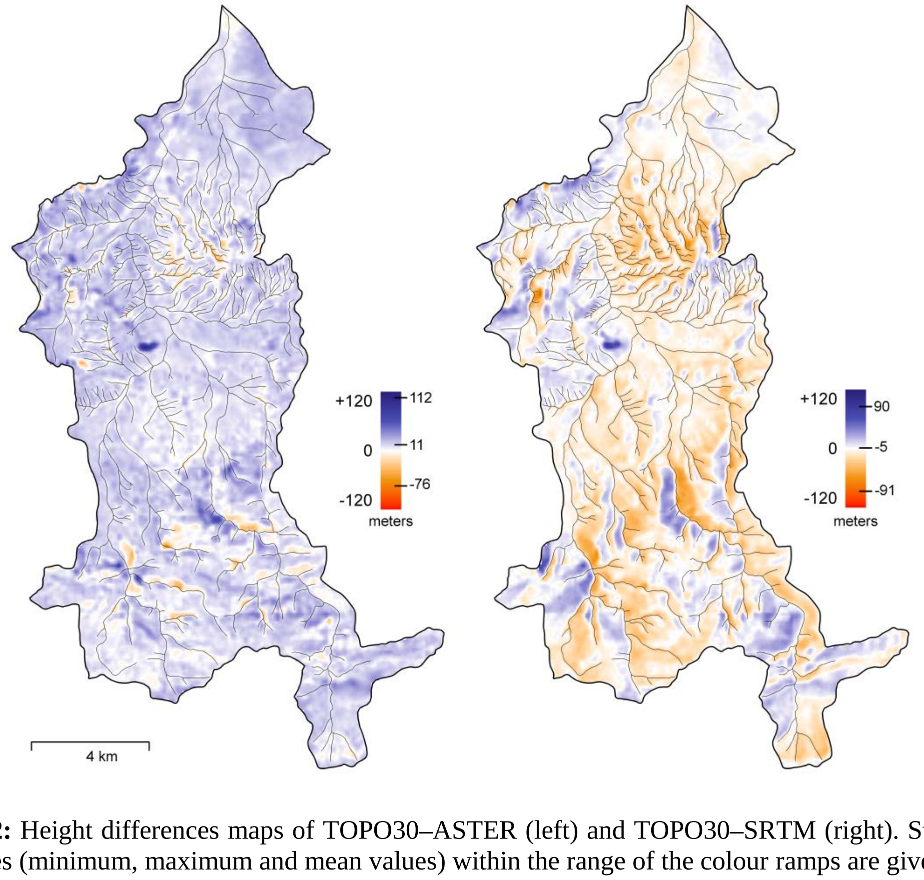

Figure 2: Height differences maps of TOPO30–ASTER (left) and TOPO30–SRTM (right). Statistical properties (minimum, maximum and mean values) within the range of the colour ramps are given.

Apart from comparing directly elevation values on a pixel basis using regression analysis (linear least squares) for the entire AOI, further investigation involved the analysis of height differences (HD) between the DEMs under evaluation and the reference TOPO30. In particular, the effort was put on the identification of spatial patters in the differences maps, related to elevation, slope gradient, slope aspect and terrain classes (Fig. 3, 4, 5 and 6), primarily by visual inspection and subsequently by geostatistical analysis of the observed differences to quantitatively address correlations. The degree of influence of those parameters is expressed by the correlation coefficient R^2. Systematic deviations were considered as well, as described by the constant b of the linear regression.

Finally, a comparative analysis between HD and the outcome of the simulation of the SRTM viewing geometry was realized. Although layover and shadow areas were not directly considered in the analysis, these areas practically coincide with regions opposite to the SAR viewing direction. This argument was verified by checking the overlap between the aforementioned regions with shadow areas calculated roughly without consideration of the varying incidence angles of those SAR systems, based on shaded relief function of the GIS and setting the illumination parameters accordingly. The performed SAR imaging simulation is in more detail described in the following section.

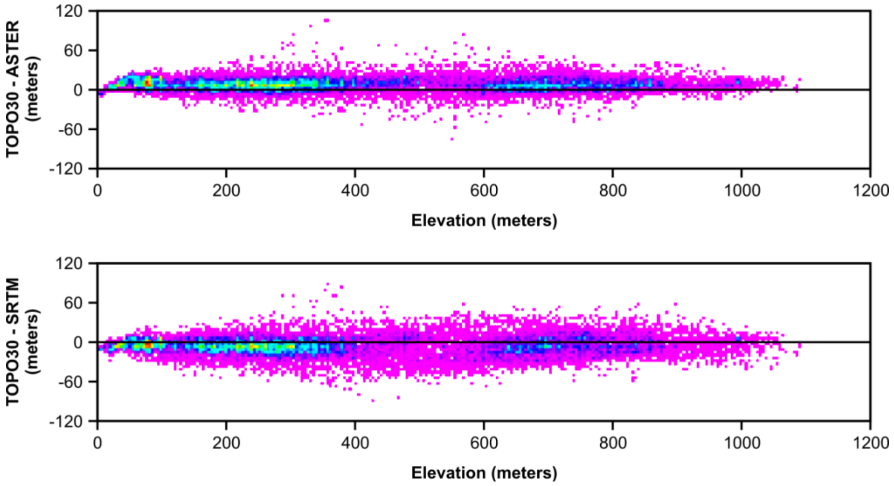

Figure 3: Scatter plots of height differences of TOPO30–ASTER (up) and TOPO30–SRTM (down) versus elevation.

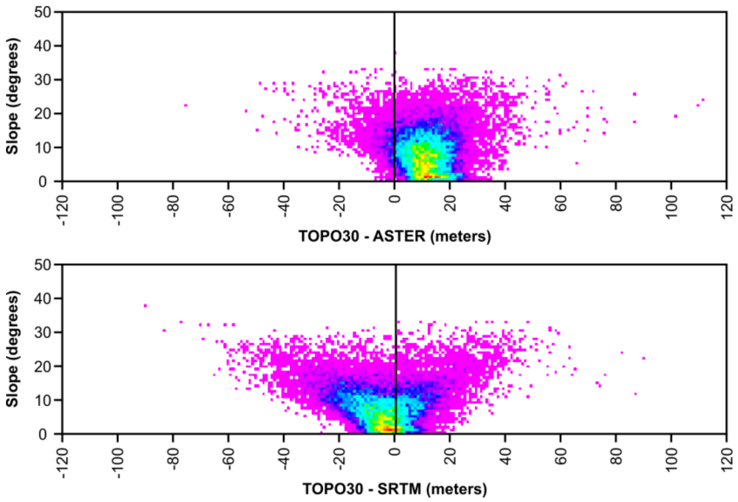

Figure 4: Scatter plots of height differences of TOPO30–ASTER (up) and TOPO30–SRTM (down) versus slope gradient.

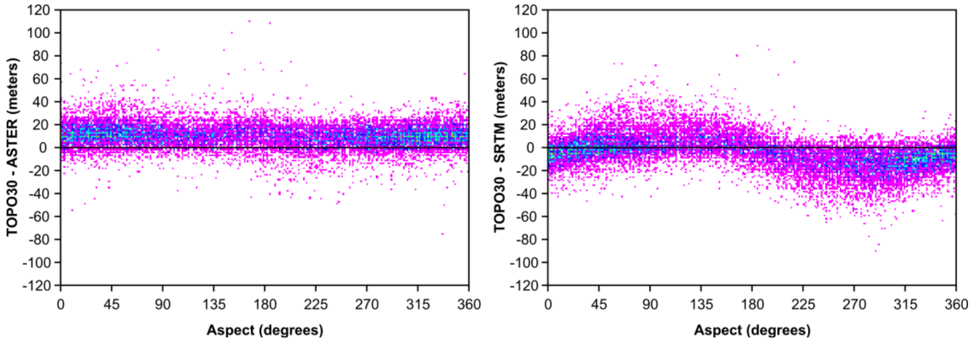

Figure 5: Scatter plots of height differences of TOPO30–ASTER (left) and TOPO30–SRTM (right) versus aspect.

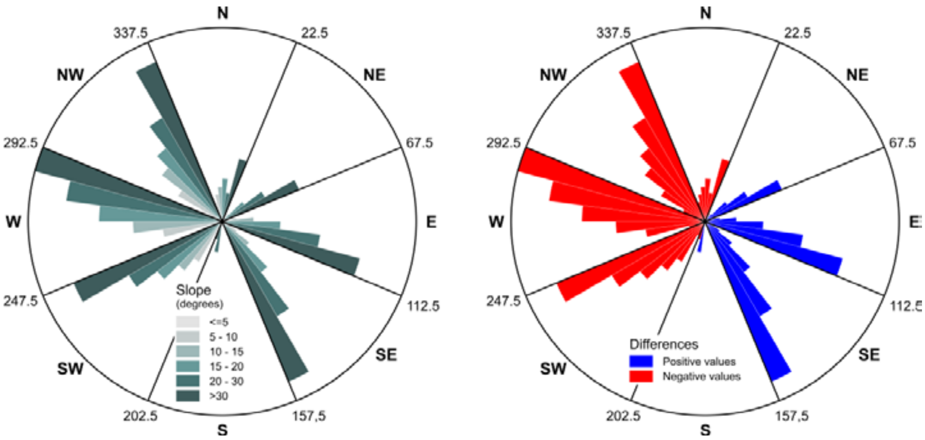

Figure 6: Relation of mean height differences and slope gradient within classes of aspect for SRTM. Positive and negative differences indicate under- and over-estimation of heights, respectively.

4. SRTM Imaging Geometry Simulation

In order to facilitate further investigation of the source of spatial deviations trends in satellite height models, a SAR simulation procedure proposed by Plank et al. (2012) was adopted accordingly. The simulation was originally developed to investigate the suitability of the Differential SAR Interferometry (DInSAR) technique for landslide monitoring prior to the radar recording of an area. Results of the simulation are (I) the accurate prediction of the areas which will be affected by layover and or shadowing and (II) the percentage of measurability of movement of a certain landslide (Fig. 7).

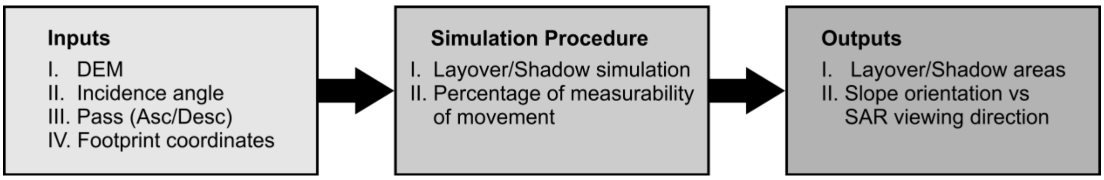

Figure 7: SRTM imaging geometry simulation steps, including inputs and outputs.

The simulation is based on (I) a digital elevation model (DEM) of the AOI and certain parameters describing the imaging geometry of the SAR satellite: (II) the incidence angle (at near range and at far range), the angle the satellite illuminates the Earth's surface, (III) the passing direction of the satellite (ascending or descending orbit) and (IV) the coordinates of the footprint, the area which is recorded by the satellite. The most critical factor regarding the accuracy of the simulation results is the spatial resolution and spatial accuracy of the DEM (Plank et al. 2012).

Here, based on the imaging geometry of SRTM, the simulation is used to (I) determine the areas which are affected by layover and or shadowing and (II) – based on a byproduct of the simulation – to identify for each part of the AOI the relationship between the SAR satellite viewing direction and the slope's dip direction, i.e. whether a certain slope is oriented averse to the satellite (in SAR viewing direction) or towards the satellite. As the final DEM provided by the SRTM mission is a combination of data acquired by an ascending pass and data from a descending pass, the simulation was applied for both imaging geometries. Thereby, we were able to classify the AOI into four categories:

1. Slopes those are averse to the SAR satellite (in SAR viewing direction) at both ascending and descending pass.
2. Regions which face the SAR satellite (i.e. towards SAR) at both ascending and descending pass.
3. Regions being in SAR viewing direction (averse) at the ascending pass and oriented towards the SAR satellite at the descending pass.
4. Slopes oriented towards the SAR satellite at the ascending pass and in SAR viewing direction at the descending pass.

The simulations were initially performed separately for each imaging geometry (ascending and descending) of the SRTM mission, outlining the regions viewing towards (To SAR view) and opposite (In SAR view) to the SAR scanning direction (Line-of-Sight, LOS). In a following step the individual results were merged into a single simulated SAR viewing map, depicting all possible combinations (Fig. 8). This procedure is in agreement with the collection and processing of SRTM data as described in Rosen et al. (2001).

5. Results and Interpretation

Based on the linear regression of heights high degrees of correlation were found for both ASTER and SRTM models, reaching 0.998 and 0.996, respectively. In general, correlation coefficients are reduced with the increase of slope gradient. The decrease is more prominent for SRTM varying approximately from 0.96 to 0.99, while the lowest values (over high relief) and the highest (over gentle slopes) for ASTER ranges between 0.98 and 0.99, respectively. The above mentioned remark is also depicted by the reduced correlation for specific terrain classes; in particular, channels and ridges (0.96). Relatively highest values are obtained over flat areas (0.99), whereas the lowest for concave and convex breaks (0.94).

Moving to height differences, an overall observation could be made regarding the sign of observed deviations/differences. Specifically, it could be seen from visual inspection that for ASTER, positive differences are dominant, showing an overall underestimation of heights (Fig. 2). On the contrary, for SRTM both signs are equally distributed, indicating both over- and under-estimations of heights within the AOI, though underestimated areas are slightly higher (Fig. 2).

A systematic underestimation of absolute heights of about 12 m on average for ASTER was shown, while for SRTM there is an overestimation with a similar systematic behaviour of approximately 5 m (Fig. 3). These average values are still within the theoretical error margin described in the products' specifications. Locally, the observed deviations from the reference DEM exceed the nominal RMSE for both datasets. The range of differences, however, should be carefully interpreted as they might correspond to real difference between the datasets. It should be kept in mind that space-borne height models, like ASTER and SRTM, illustrate the actual up-to-date topography, contrary to cartographic data which correspond to the period of their release, usually a few decades behind. In this sense, outliers in favour of TOPO30 might be related to topographical changes due to anthropogenic activities (open quarries and construction sites). Those common in both TOPO30–ASTER and TOPO30–SRTM height difference maps, recognised in the central part of the AOI, correspond to such cases (Fig. 2).

In fact, ASTER tends to overestimate valley-floor elevation and underestimate ridge elevation. Comparable tendency appears also in the SRTM data but with much higher deviations. The dependence of SRTM heights to morphological gradient is apparent, contrary to the ASTER data where no such trend is recognized (Fig. 4). It is interesting to underline that for SRTM both positive and negative signs are involved, a fact that could lead to misinterpretations when examining statistical mean values as difference at least in that case tend to average close to zero.

Although slope appears to a significant impact on HD, the observed spatial patterns cannot be entirely attributed to effect of slope (Fig. 2 and 4). Detailed examination of the HD between TOPO30 and SRTM reveal a spatial pattern related to the sign of HD in either side of valleys and ridges, a fact implying definite control of aspect for the entire AOI (Fig. 2 and 5). In other words, the majority of deviations are located in specific aspect directions, while the magnitude of deviations simply increases with the slope gradient. More specifically, it is evident that E-SE and W-NW facing slopes accommodate the largest HD for underestimated and overestimated heights, respectively (Fig. 6).

The impact of slope and aspect on the SRTM height model could be sufficiently attributed to the side viewing geometry of the SAR system (LOS observations), resulting in the recognised spatial patterns. Based on the performed simulation, it is shown that HD appears correlated to specific zones and in particular when any combination of different viewing directions is combined, namely opposite and towards the observed SAR LOS from ascending and descending orbital passes (Fig. 8). In more detail, positive deviations expressing underestimation by SRTM are mostly found on E-SE facing slopes where towards SAR view is obtained in descending and opposite in ascending orbits. For negative deviations attributed to overestimation by SRTM, the situation is exactly the reverse with towards view obtained in ascending and opposite in descending passes.

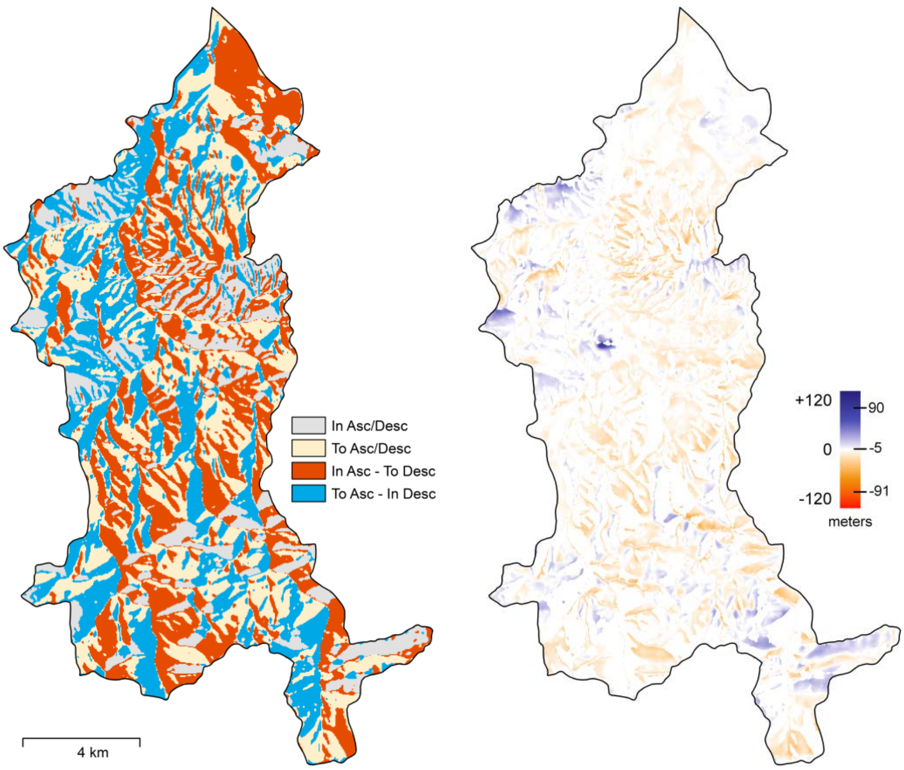

Figure 8: Simulation of SRTM imaging showing regions of different view directions, opposite or towards the SAR sensor, for combined ascending and descending orbital passes. Height deviation residuals after masking regions of alternating view from ascending and descending passes as derived by the SRTM acquisitions geometry simulation.

6. Conclusion and Discussion

The investigation of deviations in space-borne height models was one of the main focuses of the present study. Apart from quantifying these deviations in terms of a single global value, providing overall accuracy estimates, the dependency of these deviations to various geomorphological and acquisitions related factors was investigated.
From the statistical analysis performed, exploiting height errors of ASTER and SRTM models relative to a reference DEM derived from topographic data, systematic global offsets where recognized in both datasets, with relatively higher values for ASTER.
Morphological features seem to control indirectly the pattern of HD within the study area. The dependency to slope gradient and generally to high relief is more evident in SRTM. On the contrary, for the ASTER model no similar aspect related dependency was found, whereas slope dependencies are less pronounce.
On the other hand, ASTER errors could be possibly attributed to the insufficient determination of the satellite orbits and as a consequence the platform height during image acquisition. Even an error of a centimetre-level could introduce considerable offsets when resolving heights over hundred kilometres. On the other hand, SRTM data do not suffer from such source of error and thus systematic discrepancies tend to maintain relatively lower values. In that case however, the main limitations derive from the acquisition geometry and the characteristics of SAR imagery themselves, leading to a dependency to slope orientation, which in its turn is amplified by relief.
Due to the spatially varying distribution of deviations in SRTM further investigation by simulating the imaging geometry of the SRTM mission was considered. Based on the performed quantitative analysis, it was shown that regions having similar viewing geometry in both ascending and descending passes, either opposite or towards the sensor present limited deviations, -1.5 m for opposite and -5.6 m for towards to the sensor view. However, when there is difference in the viewing direction between the ascending and the descending pass, the values of deviations are significantly larger, reaching 10.1 m for ascending towards and descending opposite views and -19.2 m for ascending opposite and descending towards directions.
From a geometrical point of view, and considering the scanning direction of SRTM's SAR sensor, E-SE and W-NW facing slopes will be directly viewed only in one of the passes, since for the other they will fall into the shadow zone being opposite to the LOS direction.
This finding is directly related to regions of low or even absence of interferometric coherence over the SRTM shadow zones in both ascending and descending passes. These are actually regions viewing opposite to the SAR LOS direction in the performed simulation. Even though a weighting procedure based on coherence levels is implemented when combining different passes, it is unavoidable that these areas will receive considerably lower weights for one of the two orbits. The final height estimates are therefore dominated by only one acquisition geometry and basically no averaging is performed. On the contrary, no similar issues are expected for gently sloping terrain and for regions viewing towards to the SAR LOS in both passes.
The above outcome was quantitatively investigated and presented in the current study and expresses one of the disadvantages of the polar orbiting SAR systems when dealing with environments of complex terrain (Eineder 2003; Zhang et al. 2012). In figure 8, the residual height differences after masking out the above mentioned regions are shown. The significant reduction of errors is apparent, though few outliers do remain mostly related to overestimated heights by non-up-to-date reference DEM over human excavations sites.
Since for ASTER the assessment revealed non-spatially correlated deviations, at least partially, correction of such systematic offset for the whole examined area should be sufficiently compensated for simply by adding or subtracting an offset to the entire dataset. This correction could be applied over an area of well-known height from topographic data or GPS measurements. As for SRTM compensation of errors is not straightforward and further investigations are required to derive with an empirical formula, validated over different settings.

In terms of potential errors for various applications, it could be argued that for ASTER the possible bias in absolute height information introduces less issue compared to the spatially correlated deviation patterns in SRTM data. On one hand, the problem would be more evident when the relative changes of relief are of interest. On the other hand, the selection of such coarse height model in principal implies that accuracy requirements are not necessary high for the specific application. In any case, being within the defined accuracy limits of the products, no major problems should be expected in practice. Indeed, these models have been successfully utilised in many demanding in terms of accuracy geohazards studies (e.g. ground deformation from InSAR).

It should be mentioned that datasets like ASTER and SRTM are height models, which do not refer by definition to the ground itself, thus, are often mentioned as Digital Terrain Models (DTM) or Digital Surface Models (DSM) in the literature. Especially in the case of SAR sensors, the shorter the wavelength of the radar the higher the deviations/differences from topographic models might be found as scattering could be located well above this level. This is more evident over densely forested regions and built-up areas. This is in addition to actual differences as a result of the contemporary nature of space-borne models. These deviations are mainly attributed to human activities (surface mining, road cuts, buildings etc.) that might be of interest for specific applications, such as height of a canopy or building heights, and not necessary attributed to inaccuracies of the dataset or the techniques.

Future work is required in order to verify the outcomes of this study over larger areas and whether they indicate a general rule for ASTER and SRTM models, which should be taken into consideration when exploiting these datasets. In addition, since the release of higher resolution space-borne height models is foreseen, such as the TanDEM-X mission, careful investigations having in mind the aforementioned findings should be undertaken.

7. Acknowledgements

The authors would like to acknowledge A. Mouratidis for his comments and suggestions that improved the manuscript.

References

Abrams M., 2000. ASTER: data products for the high spatial resolution imager on NASA's EOS-AM1 platform. International Journal of Remote Sensing, 21, 847–861.

Eineder M., 2003. Problems and solutions for the INSAR Digital Elevation Models generation of mountainous terrain. Proceedings of FRINGE workshop, ESA SP-550, 1 – 5 December, Frascati, 2003.

ERSDAC, 2003. ASTER Reference Guide Version 1.0. Earth Remote Sensing Data Analysis Center, Japan, 61p.

Foumelis M., 2004. Use of Geographic Information Systems and Remote Sensing for landslide and flood susceptibility mapping. MSc Thesis, Dept. Dynamics, Tectonics & Applied Geology, National and Kapodistrian University of Athens, Athens, 243p.

Gómez-Gutiérrez A., Schnabel S., Contador F.L. and Marín R.G., 2011. Testing the quality of open-access DEMs and their derived attributes in Spain: SRTM, GDEM and PNOA DEM. Geomorphometry, 53–56.

Gorokhovich Y. and Voustianiouk A., 2006. Accuracy assessment of the processed SRTM-based elevation data by CGIAR using field data from USA and Thailand and its relation to the terrain characteristics. Remote Sensing of Environment, 104(4), 409–415, doi:10.1016/j.rse.2006.05.012.

Hirano A., Welch R. and Lang H., 2003. Mapping from ASTER stereo image data: DEM validation and accuracy assessment. ISPRS Journal of Photogrammetry & Remote Sensing, 57, 356-370.

Hutchinson M.F., 1989. A new procedure for gridding elevation and stream line data with automatic removal of spurious pits. Journal of Hydrology, 106, 211-232.

Hutchinson M.F., 1993. Development of a continent-wide DEM with applications to terrain and climate analysis. In: M.F. Goodchild et al. (eds), Environmental Modeling with GIS, New York, Oxford University Press, 392-399.

Lee H.-Y., Kim T., Park W. and Lee H.-K., 2003. Extraction of digital elevation models from satellite stereo images through stereo matching based on epipolarity and scene geometry. Image and Vision Computing, 21, 789–796.

Miliaresis G.C., 2007. An upland object based modelling of the vertical accuracy of the SRTM-1 elevation dataset. Journal of Spatial Science, 52(1), 13-28, doi:10.1080/14498596.2007.9635097.

Miliaresis, G.C., 2008. The Landcover Impact on the Aspect/Slope Accuracy Dependence of the SRTM-1 Elevation Data for the Humboldt Range. Sensors, 8, 3134-3149; doi:10.3390/s8053134.

Mouratidis A., Briole P. and Katsambalos K., 2010. SRTM 3″ DEM (versions 1, 2, 3, 4) validation by means of extensive kinematic GPS measurements: a case study from North Greece. International Journal of Remote Sensing, 31(23), 6205-6222, doi:10.1080/01431160903401403.

Nikolakopoulos K.G. and Chrysoulakis N., 2006. Updating the 1:50.000 topographic maps using ASTER and SRTM DEM. The case of Athens, Greece. Remote Sensing for Environmental Monitoring, GIS Applications, and Geology VI, edited by Manfred Ehlers, Ulrich Michel, Proc. of SPIE vol. 6366, 636606, doi:10.1117/12.689016

Nikolakopoulos K.G., Kamaratakis E.K., and Chysoulakis N., 2006. SRTM vs ASTER elevation products. Comparison for two regions in Crete, Greece. International Journal of Remote Sensing, 27(21), 4819-4838.

Plank S., Singer J., Minet C. and Thuro K., 2012. Pre-survey suitability evaluation of the differential synthetic aperture radar interferometry method for landslide monitoring. International Journal of Remote Sensing, 33(20), 6623-6637.

Rabus B., Eineder M., Roth A. and Bamler R., 2003. The shuttle radar topography mission—a new class of digital elevation models acquired by spaceborne radar. ISPRS Journal of Photogrammetry & Remote Sensing, 57, 241– 262.

Rawat K.S., Mishra A.K., Sehgal V.K., Ahmed N. and Tripathi V.K., 2013. Comparative evaluation of horizontal accuracy of elevations of selected ground control points from

ASTER and SRTM DEM with respect to CARTOSAT-1 DEM: a case study of Shahjahanpur district, Uttar Pradesh, India. Geocarto International, 28(5), 439-452, doi:10.1080/10106049.2012.724453.

Rodríguez E., Morris C.S., Belz J.E., Chapin E.C., Martin J.M., Daffer W. and Hensley S., 2005. An Assessment of the SRTM Topographic Products. Technical Report D-31639, Jet Propulsion Laboratory, Pasadena, California, 143p.

Rosen P., Eineder M., Rabus B., Gurrola E., Hensley S. Knöpfle W., Breit H., Roth A. and Werner M., 2001. SRTM Mission – Cross Comparison of X and C Band Data Properties. Proceedings of IGARSS, Sydney, Australia, unpaginated CD-ROM.

Sharma A., Tiwari K.N. and Bhadoria P.B.S., 2010. Vertical accuracy of digital elevation model from Shuttle Radar Topographic Mission – a case study. Geocarto International, 25(4), 257-267, doi:10.1080/10106040903302931.

Shortridge A. and Messina J., 2011. Spatial structure and landscape associations of SRTM error. Remote Sensing of Environment, 115(6), 1576–1587, doi:10.1016/j.rse.2011.02.017.

Travis M.R., Elsner G.H., Iverson W.D., Johnson C.G., 1975. VIEWIT computation of seen areas, slope and aspect for land-use planning. U.S. Dept. of Agriculture Forest Service Gen. Techn. Rep. PSW 11/1975, Pacific Southwest Forest and Range Experimental Station, Berkley, California, 70p.

Van Niel T.G., McVicar T.R., Li L-T., Gallant J.C. and Yang Q-K., 2008. The impact of misregistration on SRTM and DEM image differences. Remote Sensing of Environment, 112(5), 2430–2442, doi:10.1016/j.rse.2007.11.003.

Werner M., 2001. Status of the SRTM data processing: when will the world-wide 30m DTM data be available? In: Geo-Informationssysteme, Heidelberg: Herbert Wichmann/Hüthig, 6–10.

Zhang W., Weihong Wang W. and Chen L., 2012. Constructing DEM Based on InSAR and the Relationship between InSAR DEM's Precision and Terrain Factors. Energy Procedia, 16(A), 184–189, doi:10.1016/j.egypro.2012.01.031.